

Scanning Tunneling Microscopy and Spectroscopy of Wet-Chemically Prepared Chlorinated Si(111) Surfaces

Peigen Cao, Hongbin Yu,[†] and James R Heath*

Division of Chemistry and Chemical Engineering, Noyes Laboratory, 127-72, Kavli Nanoscience Institute, California Institute of Technology, Pasadena, California 91125

Received: July 10, 2006; In Final Form: September 5, 2006

Chlorine-terminated Si(111) surfaces prepared through the wet-chemical treatment of H-terminated Si(111) surfaces with PCl_5 (in chlorobenzene) were investigated using ultrahigh vacuum scanning tunneling microscopy (UHV cryo-STM) and tunneling spectroscopy. STM images, collected at 77 K, revealed an unreconstructed 1×1 structure for the chlorination layer, consistent with what has been observed for the gas phase chlorination of H-terminated Si(111). However, the wet-chemical chlorination is shown to generate etch pits in the Si(111) surface, with an increase in etch pit density correlating with increasing PCl_5 exposure temperatures. These etch pits were assumed to stabilize the edge structure through the partial removal of the $\langle 11\bar{2} \rangle$ step edges. Tunneling spectroscopy revealed a nonzero density of states at zero bias. This is in contrast to the cases of H-, methyl-, or ethyl-terminated Si(111), in which similar measurements have revealed the presence of a large conductance gap.

Introduction

Functionalization of Si(111) surfaces with covalently bonded organic reagents has attracted interest as a method for tailoring the chemical and electrical properties of Si surfaces.^{1–5} In particular, alkyl passivated Si(111) surfaces prepared through a two-step chlorination/alkylation route^{3–5} have shown low charge-carrier surface recombination velocities, oxidation resistance in air and during anodic current flow in electrochemical cells, and a number of other interesting chemical and electronic properties. The chlorinated Si(111) surface ($\text{Cl}/\text{Si}(111)$) is a key intermediate in this chemistry. Surface chemical component analysis of $\text{Cl}/\text{Si}(111)$ has been performed using X-ray photoelectron spectroscopy,^{5,6} infrared,⁷ and high-resolution electron energy loss spectroscopy,⁸ indicating formation of the $\text{Cl}-\text{Si}$ bond. The expected 1×1 structure of the chlorination layer was confirmed in a recent scanning tunneling microscopy study of the $\text{Cl}/\text{Si}(111)$ surface prepared by the gas phase reaction of H/Si(111) with molecular chlorine.⁸ $\text{Cl}-\text{Si}$ bond-induced stacking faults were previously observed by Itchkawitz et al.⁹ That report was based upon the observation that inequivalent crystallographic directions ($\langle 1\bar{1}2 \rangle$ and $\langle 11\bar{2} \rangle$) were found to exhibit the same bilayer step edge structure. In addition, significant enhancement of surface conductance for $\text{Cl}/\text{Si}(111)$ was reported by Lopinski et al.¹⁰ A p-type inversion layer was used to interpret this effect in terms of the formation of a 2D hole gas.

The morphology of a chlorinated Si(111) surface is apparently dependent upon the nature of the chemistry utilized for that chlorination, and that is the hypothesis that we test in this paper. For example, when a H/Si(111) surface that is characterized by

a low density of step edges is halogenated via the reaction with gas phase molecular chlorine, the resultant $\text{Cl}/\text{Si}(111)$ surface remains extremely flat.⁸ However, when a similarly flat H/Si(111) is chlorinated via the reaction with PCl_5 in chlorobenzene solution and subsequently alkylated, the resultant alkyl/Si(111) is characterized by a high density of etch pits, with a corresponding large fraction of alkylated Si atoms residing at the edge of those pits.^{11,12} Those atoms are more chemically accessible than the alkylated Si atoms that reside on terraces, and thus can play a role in subsequent chemical processes on the surface.¹³ They can also play important roles in driving the formation of a stacking fault.¹¹

The etch pits presumably originate during the chlorination procedure. In this Letter, we report on the scanning tunneling microscopy (STM) and tunneling spectroscopy (STS) of wet-chemically prepared $\text{Cl}/\text{Si}(111)$ surfaces. We show that this wet-chemical chlorination of H/Si(111) does, in fact, introduce a large density of etch pits of one or more atomic steps in depth. Nevertheless, Cl atoms still passivate 100% of the atop Si atom sites on the unreconstructed Si(111) surface. The etch pits result in fragmented $\langle 11\bar{2} \rangle$ steps and do not lead to stacking faults on the chlorinated surface. Unlike the cases for H/Si(111), methyl/Si(111), or ethyl/Si(111),¹⁴ tunneling spectroscopy revealed the absence of a band gap: current–voltage traces exhibited a nonzero slope at zero applied bias, implying a nonzero density of states (DOS) at the Fermi level.

Experimental Section

The substrates utilized were (111)-oriented, Sb-doped, n-type Si wafers with a low miscut angle of $\pm 0.5^\circ$ and a resistivity of $0.005\text{--}0.02 \, \Omega \cdot \text{cm}$. A standard RCA cleaning process was used to prepare the samples. Briefly, the substrate was immersed in a basic peroxide solution which is composed of 1:1:4 by volume

* Corresponding author. E-mail: heath@caltech.edu.

[†] Current address: Department of Electrical Engineering, ERC 159, Mail Code 5706, Arizona State University, Tempe, AZ 85287-5706.

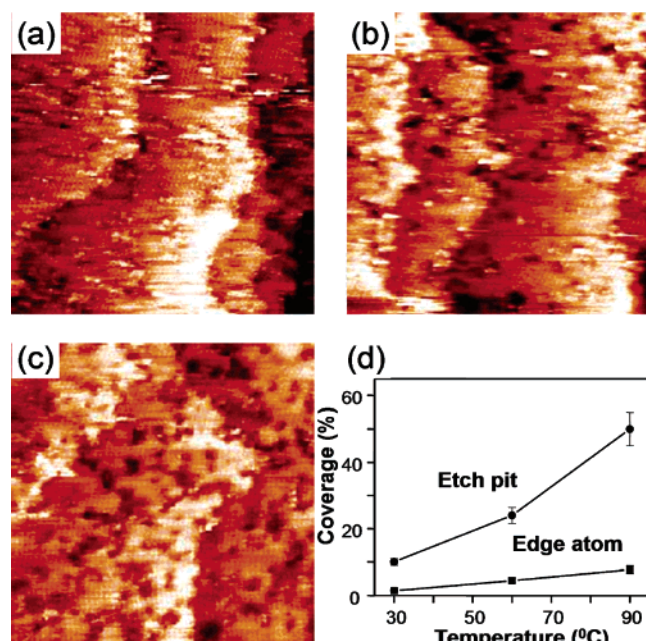


Figure 1. (a–c) Constant-current STM images of the Cl/Si(111) surfaces prepared at different temperatures—(a) 30 °C, 5 h; (b) 60 °C, 3 h; (c) 90 °C, 50 min—acquired at a sample voltage of -1.0 V. Scan area = 100×100 nm. (d) Plot of etch pit and edge atom coverage against reaction temperature.

28% $\text{NH}_3 \cdot \text{H}_2\text{O}(\text{aq})/30\%$ $\text{H}_2\text{O}_2/\text{H}_2\text{O}$ at 80 °C for at least 10 min and then rinsed thoroughly in running Milli-Q water. H/Si(111) was formed by immersing the cleaned sample in 40% NH_4F for 15 min. This step produces large, atomically flat terraces.¹⁵ Chlorination was performed in a nitrogen-purged glovebox. A few grains of benzoyl peroxide were added to a saturated solution of PCl_5 in chlorobenzene, and the solution was then heated to 90–100 °C for 50 min. For lower temperature experiments, the reaction time was adjusted so that a complete chlorination of the Si surface was reached. This was monitored by the surface conductivity test, since the conductivity was observed to increase significantly in comparison with H/Si. After the reaction, the sample was removed from the solution and rinsed thoroughly with tetrahydrofuran. The samples were then dried under a streaming $\text{N}_2(\text{g})$, mounted onto a sample stage, and quickly introduced into an Omicron low-temperature ultrahigh vacuum (UHV) STM system. Both imaging and spectroscopy data were acquired at 77 K by use of mechanically cut or etched Pt–Ir tips. Tunneling spectroscopy was acquired by fixing the tip–sample distance at a specified bias voltage and a set current with feedback off.

Results and Discussion

Figure 1a–c shows constant-current STM images of the Cl/Si(111) surfaces prepared at three temperatures. The etch hillocks of a single bilayer step in depth are clearly seen and are pointing to the $\langle 1\bar{1}2 \rangle$ orientation. In comparison with the H/Si(111),¹⁵ an obvious increase in etch pit density was observed for Cl/Si(111) prepared at all three temperatures. These etch pits are of one or more bilayer steps in depth. Previous results from methylated and ethylated Si(111) surfaces displayed a similar etch pit morphology,¹⁶ although again with atomically flat terraces. The conclusion is that the increased etch pit density is most certainly caused by the wet-chemical chlorination procedure. Since the step sites are expected to be more chemically accessible than the terrace sites, the chlorination chemistry essentially transforms these relatively inert terrace

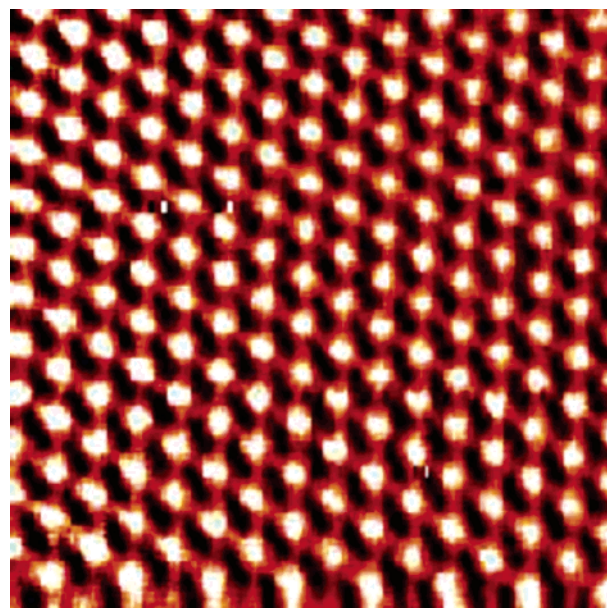


Figure 2. Constant-height STM image of a surface prepared at 90 °C showing uniform Cl atom coverage on the atop sites of the unreconstructed surface. Scan area = 5×5 nm, $V_b = -0.8$ V, $I_t = 0.27$ nA.

sites to more reactive step sites which can be exploited in subsequent chemical reactions. It may thus be possible to tailor the surface chemical activity by changing the terrace-to-step site ratio via control over the chlorination chemistry. The etching chemistry could, in fact, be modified by changing the reaction temperature (Figure 1). The coverage of etch pit and edge atom were quantified (see the Supporting Information) and plotted versus temperature in Figure 1d. An increase in reaction temperature led to an increase in both etch pit coverage and step-to-terrace ratio. A dependence of etch pit density upon the reaction conditions was also observed for Cl/Si(111) prepared via reactions of H/Si(111) with $\text{Cl}_2(\text{g})$. Under UV irradiation and at room temperature, Lopinski and co-workers¹⁰ prepared Cl/Si(111) surfaces with a considerable number of etch pits by reaction with molecular chlorine, whereas the reaction without UV irradiation resulted in a completely flat surface with few etch pits.⁸ The surface morphology is apparently dependent upon the relative etch rates of the terraces, step edges, kinks, and other surface structures. The large number of etch pits in the Cl/Si(111) surface observed on surfaces prepared at higher temperatures is likely ascribable to the increased ratio of the terrace etch rate to the kink etch rate.

In spite of the increased number of etch pits in the chlorinated surface, a full coverage of Cl–Si on the Si(111) atop sites could be achieved through the solution phase chemical approach. This 100% coverage is suggested by the constant-height atomic-resolution image, as shown in Figure 2, and by experiments in which methyl and acetyl Grignard reagents have been shown to fully alkylate such a chlorinated surface.^{13,16} Constant-current-mode images, at this resolution, were of slightly poorer quality but still revealed the full coverage and hexagonal structure of the Cl–Si on the surface. While it would have been interesting to obtain an image of a step edge at a similarly high resolution to that presented in Figure 2, such an image would require constant-current-mode imaging. Statistical analysis of the nearest-neighbor-atom distances revealed a peak value of ~ 3.8 Å, which is the distance between silicon atop sites on the unreconstructed Si(111) surface.¹⁷ This suggests an unreconstructed 1×1 structure and hence a full passivation of the atop Si atoms by Cl, consistent with reported results from the gas

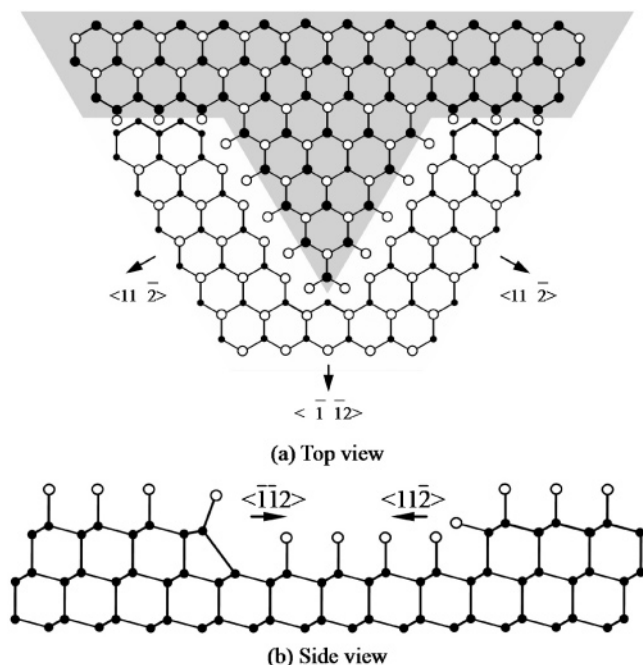


Figure 3. Schematics of the $\langle 11\bar{2} \rangle$ and $\langle \bar{1}12 \rangle$ step terminating structure for chlorinated Si(111) surfaces.

phase chlorination of H-terminated Si(111).⁸ Similar images were obtained from other terrace sites. Atomically flat surfaces with a minimal amount of contamination can be identified from the image, indicating that the wet-chemically prepared Cl/Si(111) can survive at least moderate postprocessing conditions that include a several minute air exposure prior to introduction into the UHV STM chamber.

Another interesting set of observations are the fragmented $\langle 11\bar{2} \rangle$ steps with the outward normal along the $\langle 11\bar{2} \rangle$ orientation. Figure 3a is an illustration of the etch hillock observed in STM images. For H/Si(111) surfaces, it has been shown that a $\langle 11\bar{2} \rangle$ step is terminated by the lower Si atoms of the bilayer, forming a horizontal monohydride termination structure.¹⁵ By contrast, $\langle \bar{1}12 \rangle$ steps are terminated by the upper Si atoms, resulting in a vertical dihydride structure.¹⁵ Upon chlorination, a rebonded step geometry was formed at the $\langle \bar{1}12 \rangle$ steps, where the step terminating Si atoms are bonded to the bottom terrace silicon atoms (see Figure 3b).⁹ The full chlorination of the $\langle 11\bar{2} \rangle$ step terminating Si atoms has been shown to be energetically unfavorable. This might be attributed to the significant electrostatic repulsion between the negatively charged chlorine atoms along the upper and lower terraces of the $\langle 11\bar{2} \rangle$ steps.⁹ Periodic DFT calculations indicated that the Si–Cl bond on

$\langle \bar{1}12 \rangle$ is 0.58 eV stronger than that on $\langle 11\bar{2} \rangle$. For CH₃/Si(111), the difference is even greater (0.67 eV).¹¹

A stacking fault basically switches a $\langle 11\bar{2} \rangle$ step to a $\langle \bar{1}12 \rangle$ step. Calculations indicated that a full stacking fault on the terraces is energetically possible for etched CH₃/Si(111) and Cl/Si(111) surfaces. Partly faulted regions were observed by Itchckawitz et al. on the Cl/Si(111) and were inferred for CH₃/Si(111) by us through a combination of experiment¹⁶ and theory.¹¹ For our Cl/Si(111) surfaces prepared at 90 °C, the terrace-to-step site ratio (estimated to be ~ 13 from the STM images) indicates that stacking faults would be energetically possible.¹¹ However, no stacking faults were observed for any of our preparations. Careful inspection of the etch hillock edges (Figure 1c) revealed that the $\langle 11\bar{2} \rangle$ step edges were actually segmented, or further etched. An etched $\langle 11\bar{2} \rangle$ step edge site creates two kink sites, each of which possesses the $\langle \bar{1}12 \rangle$ step edge structure. This further etching therefore partially removes the $\langle 11\bar{2} \rangle$ step edge atoms and essentially changes the $\langle 11\bar{2} \rangle$ step structure to the $\langle \bar{1}12 \rangle$ step structure, thus stabilizing the surface.

We also investigated the tunneling spectroscopy of wet-chemically prepared Cl/Si(111). Current–voltage traces, averaged over the area shown in Figure 2, are represented in Figure 4a, together with a similarly averaged trace collected from H/Si(111). The set points for bias voltage and current were experimentally varied. For the data shown in Figure 4, the experimental values were -0.8 V and 0.27 nA for Cl/Si(111) and -1.7 V and 0.12 nA for H/Si(111).

Fully passivated H/Si(111) exhibits a large conductance gap. This gap, which did decrease slightly upon a decrease of the bias voltage, exhibited a limiting value of 1.6 V at a bias voltage of -1.7 V. Similarly large conductance gaps have been recently reported for methyl/Si(111) (100% passivation) and ethyl/Si(111) (80% ethyl-; 20% H-passivation).¹⁴ This has been attributed to the absence of surface states for these chemically functionalized surfaces. Additionally, tip-induced band bending might also contribute to the observed, relatively broad conductance gap.¹⁸

The current–voltage characteristics of Cl/Si(111) exhibited no evidence of a band gap (see Figure 4a), with the I – V curve possessing a finite slope at zero bias voltage. Varying the bias voltage in a range of -1.5 to -0.3 V yielded consistent results. This is indicated by a nonzero DOS at the Fermi level. From a log(current) versus voltage plot (Figure 4b), three different conductance regions are apparent. At positive values of sample voltage, a conductance response attributable to tunneling out of the tip and into the Si conduction band is observed. For negative-valued sample voltages below about -1.1 V, the

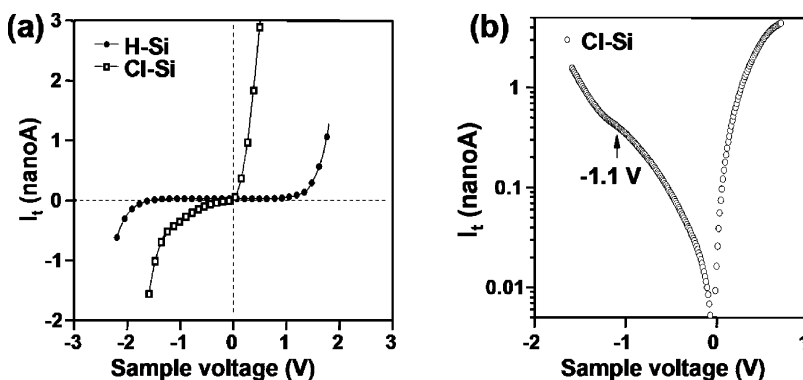


Figure 4. (a) Representative low-temperature (77 K) tunneling spectrum for H- and Cl-terminated Si(111) surfaces. (b) Logarithmic plot for Cl/Si(111). Each I – V curve is an average of 2500 I – V curves taken at different points on the surface.

current is dominated by the tunneling of the valence band electrons from the silicon into the tip. The third region is that which is bracketed by negative-valued sample biases between 0 and -1.1 V.

Since the UHV STM images show atomically flat surfaces with minimal surface contamination, the finite conductance observed at zero bias could then be explained in terms of the intrinsic Cl/Si(111) surface properties. Unlike the H-Si(111) where the Fermi level is unpinned, the strong electronegativity of chlorine was expected to induce a large upward band bending, where the Fermi level approaches the top of the valence band edge.¹⁹ Strong surface band bending induced by adsorbates such as metal and semiconductor atoms, oxygen, and halogens has been observed at even submonolayer coverages.²⁰ These adsorbates have also been shown to induce intrinsic surface states, pinning the Fermi level (E_F) at a position dependent upon the difference between the electronegativity of the adsorbate and the substrate atoms.²⁰ E_F pinning close to the edge of the valence band has been previously observed on Cl/GaAs(110) surfaces.¹⁹ Therefore, due to the large band bending, at negative sample bias near 0 V, the probability of thermionic emission of silicon conduction band electrons followed by tunneling through the vacuum barrier was expected to be low.²¹ At increasing values of forward bias, the surface barrier decreases and hence the tunneling current increases. A theoretical model of this surface would likely provide clarification of this picture. Surface recombination velocity measurements²² have revealed a low velocity for a freshly prepared Cl-Si sample, followed by a sharp increase in recombination rate upon oxidation. Interestingly, although the observation of finite conductance between 0 and -1.1 V may obscure the observation of the valence band edge, the present data do exhibit an inflection near 1.1 V (Figure 4b), which is very close to the bulk band gap value.

In summary, cryo-STM images of wet-chemically prepared Cl/Si(111) surfaces showed an unreconstructed 1×1 structure and hence full replacement of hydrogen by chlorine atoms. An increased etch pit density relative to gas phase prepared Cl/Si(111) was observed, and could be controlled experimentally. Such control may enable the tailoring of the surface chemical reactivity toward subsequent alkylation and other functionalization processes. Tunneling spectroscopy revealed a nonzero DOS near zero applied bias, in contrast to analogous measurements on H/Si(111), methyl/Si(111), and ethyl/Si(111) surfaces. This may indicate that the electronegative $-Cl$ atoms are inducing surface states which are contributing to current observed within the usual forbidden region.

Acknowledgment. The authors acknowledge the National Science Foundation, grant CHE-0213589 (NSL), NSF-CCF-05204490, and the Department of Energy (JRH) for support of this research. The authors thank Professor Nate Lewis, Rosemary Dyane Rohde, Heather Dawn Agnew, Dr. Woon-Seok Yeo, and Dr. Patrick T. Hurley for helpful discussions and technical assistance in preparation of the chlorinated silicon samples.

Supporting Information Available: Etch pit and edge atom coverage calculation steps. This material is available free of charge via the Internet at <http://pubs.acs.org>.

References and Notes

- (1) Buriak, J. M. *Chem. Rev.* **2002**, *102*, 1271.
- (2) Weldon, M. K.; Queeney, K. T.; Eng, J. Jr.; Raghavachari, K.; Chabal, Y. *Surf. Sci.* **2002**, *500*, 859.
- (3) Bansal, A.; Li, X. L.; Lauermann, I.; Lewis, N. S.; Yi, S. I.; Weinberg, W. H. *J. Am. Chem. Soc.* **1996**, *118*, 7225.
- (4) Royea, W. J.; Juang, A.; Lewis, N. S. *Appl. Phys. Lett.* **2000**, *77*, 1988.
- (5) Webb, L. J.; Nemanick, E. J.; Biteen, J. S.; Knapp, D. W.; Michalak, D. J.; Traub, M. C.; Chan, A. S. Y.; Brunschwig, B. S.; Lewis, N. S. *J. Phys. Chem. B* **2005**, *109*, 3930.
- (6) Rivillon, S.; Chabal, Y. J.; Webb, L. J.; Michalak, D. J.; Lewis, N. S.; Halls, M. D.; Raghavachari, K. *J. Vac. Sci. Technol.* **2005**, *A23*, 1100.
- (7) Rivillon, S.; Amy, F.; Chabal, Y. J.; Frank, M. M. *Appl. Phys. Lett.* **2004**, *85*, 2583.
- (8) Eves, B. J.; Lopinski, G. P. *Surf. Sci.* **2005**, *579*, L89.
- (9) Itchkawitz, B. S.; McEllistrem, M. T.; Boland, J. J. *Phys. Rev. Lett.* **1997**, *78*, 98.
- (10) Lopinski, G. P.; Eves, B. J.; Hul'ko, O.; Mark, C.; Patitsas, S. N.; Boukherroub, R.; Ward, T. R. *Phys. Rev. B* **2005**, *71*, 125308.
- (11) Solares, S. D.; Yu, H. B.; Webb, L. J.; Lewis, N. S.; Heath, J. R.; Goddard, W. A. *J. Am. Chem. Soc.* **2006**, *128*, 3850.
- (12) Yu, H. B.; Solares, S. D.; Webb, L. J.; Cao, P. G.; Lewis, N. S.; Heath, J. R.; Goddard, W. A. *J. Phys. Chem. B* **2006**, in press.
- (13) Rohde, R. D.; Agnew, H. D.; Yeo, W. S.; Heath, J. R. *J. Am. Chem. Soc.* **2006**, *128*, 9518.
- (14) Yu, H. B.; Webb, L. J.; Heath, J. R.; Lewis, N. S. *Appl. Phys. Lett.* **2006**, *88*, 252111.
- (15) Hines, M. A. *Ann. Rev. Phys. Chem.* **2003**, *54*, 29.
- (16) Yu, H. B.; Webb, L. J.; Ries, R. S.; Solares, S. D.; Goddard, W. A.; Heath, J. R.; Lewis, N. S. *J. Phys. Chem. B* **2005**, *109*, 671.
- (17) Waltenburg, H. N.; Yates, J. T., Jr. *Chem. Rev.* **1995**, *95*, 1598.
- (18) McEllistrem, M. T.; Haase, G.; Chen, D.; Hamers, R. J. *Phys. Rev. Lett.* **1993**, *70*, 2471.
- (19) Troost, D.; Koenders, L.; Fan, L. Y.; Mönch, W. *J. Vac. Sci. Technol., B* **1987**, *5*, 1119.
- (20) Mönch, W. *J. Vac. Sci. Technol., B* **1986**, *4*, 1085.
- (21) Strocio, J. A.; Feenstra, R. M. *J. Vac. Sci. Technol., B* **1988**, *6*, 1472.
- (22) Lewis, N. S. Private communication.